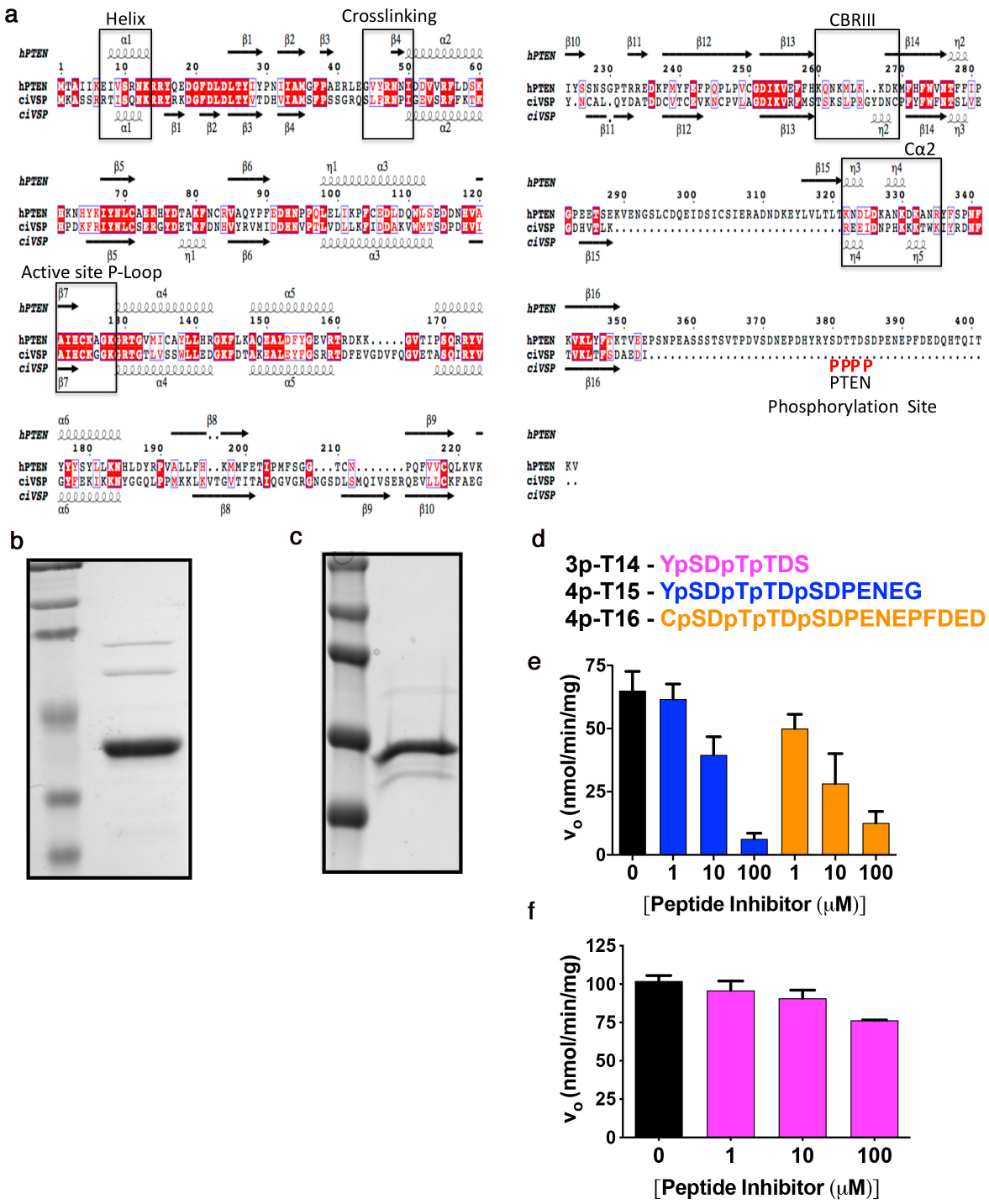

Figure S1. Engineering and evaluating a chimeric version of VSP and PTEN. a, Primary and secondary structure overlay of our new PTEN structure and VSP (PDB: 3V0D, chain B) using ESPript. b, SDS-PAGE gel showing EPL product of 4p-crPTEN-13$_{sp}$-T2. c, SDS-PAGE gel showing EPL product 4p-VSP (VSP/PTEN chimera). d, Sequence of phosphorylated peptides used in inhibition experiments. e, Bar graph of the initial velocity of PTEN in the presence of changing concentration of either 4p-T15 or 4p-T16 peptide inhibitor. Assay condition: 50 mM Tris pH 8.0, 100 mM NaCl, 10 mM 2-mercaptoethanol. f, Bar graph of the initial velocity of PTEN in the presence of changing concentration of 3p-T14 peptide inhibitor. Assay condition: 50 mM Tris pH 8.0, 10 mM 2-mercaptoethanol. Uncertainty reported as ± SEM.

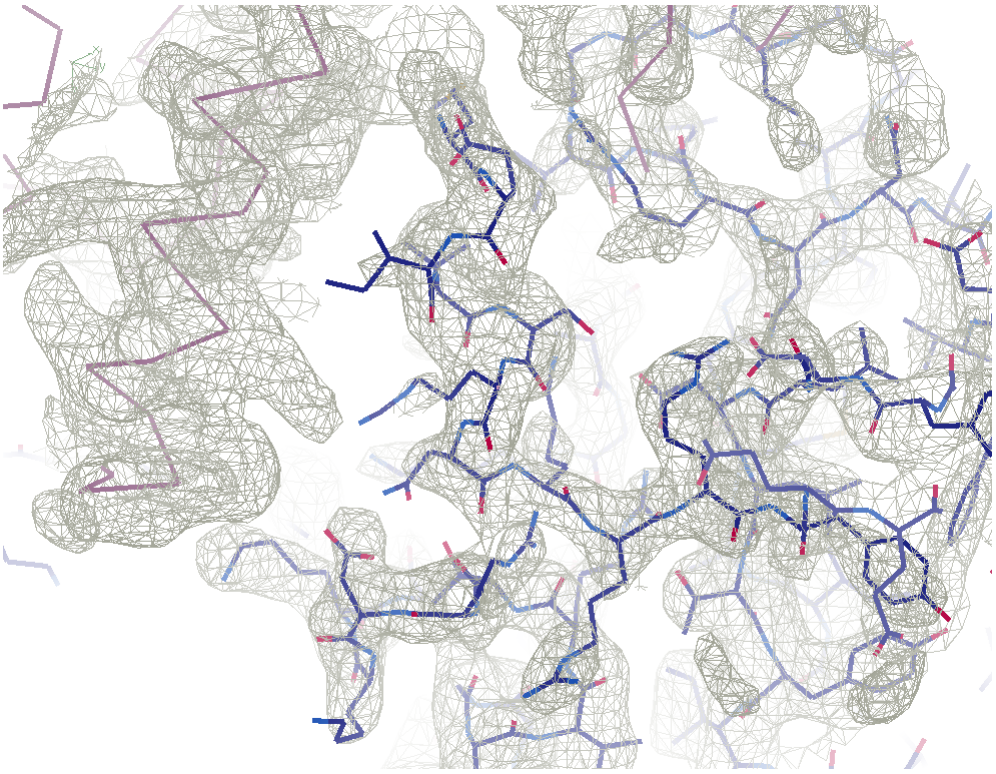

Figure S2. Composite omit map of the n-crPTEN-13sp-T1 (PDB ID 7JUL). The map is displayed at 1 σ (grey mesh) with refined structure as blue sticks and symmetry related molecules as C-alpha (dark berry).

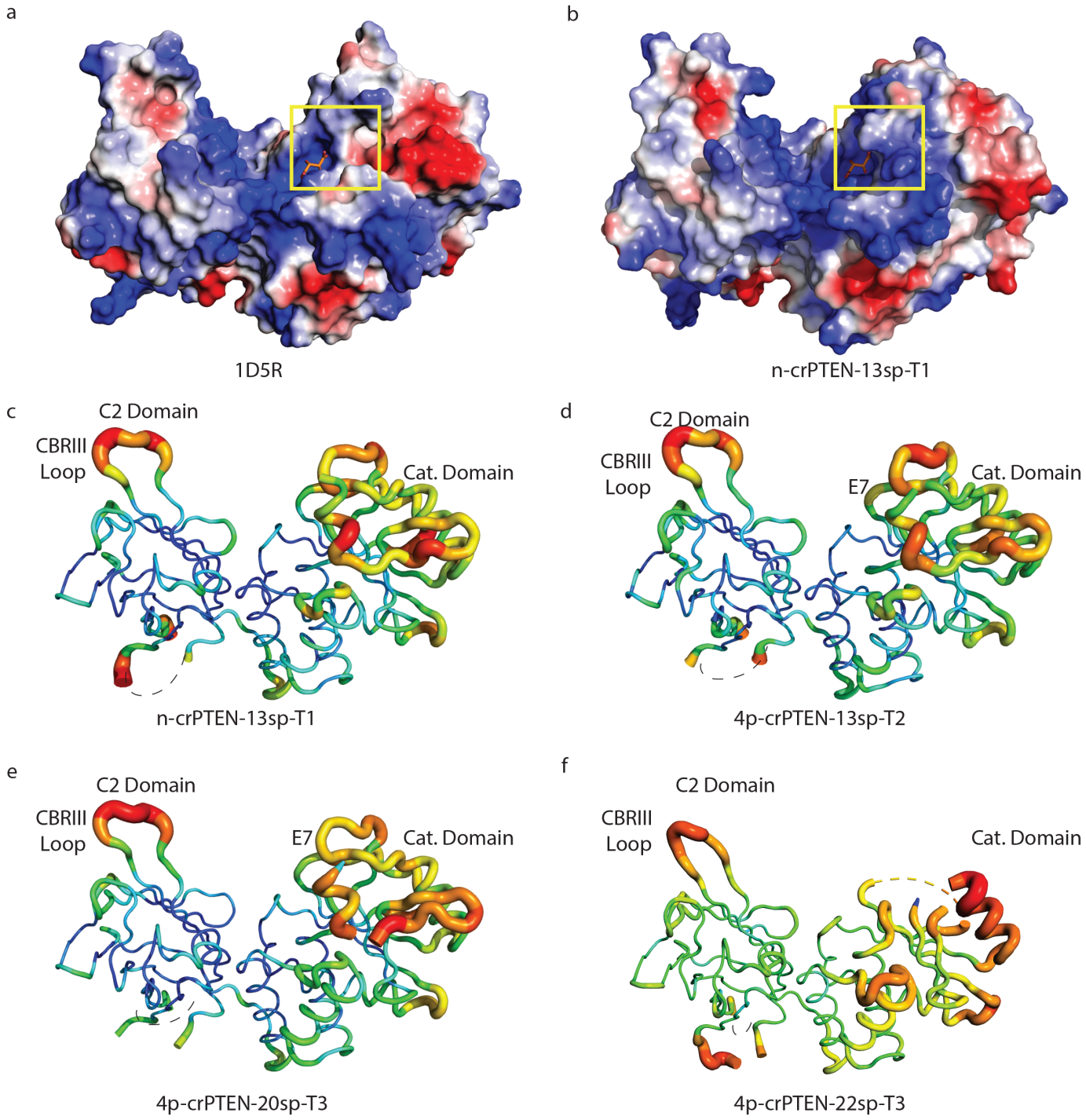

Figure S3. N-terminal Helix 1 extends a positively charged patch on PTEN. a, surface representation of PTEN 1D5R colored as the electrostatic potential with the N-terminal helix area of 4p-crPTEN-13$_{sp}$-T2 (PDB ID 7JUK) marked as a yellow box. The tartrate molecule observed in 1D5R bound to active site is shown as orange sticks. b, surface representation of 4p-crPTEN-13$_{sp}$-T2 colored as the electrostatic potential displays how the N-terminal helix closes up the tartrate binding site. c, d, e, f, structures of n-crPTEN-13sp-T1, 4p-crPTEN-13$_{sp}$-T2, 4p-crPTEN-20sp-T3, 4p-crPTEN-22sp-T3 in ribbons with the width of the tube proportional to b-factors. The N-terminal helix, loop of catalytic Domain, and CBRIII display the highest spread.

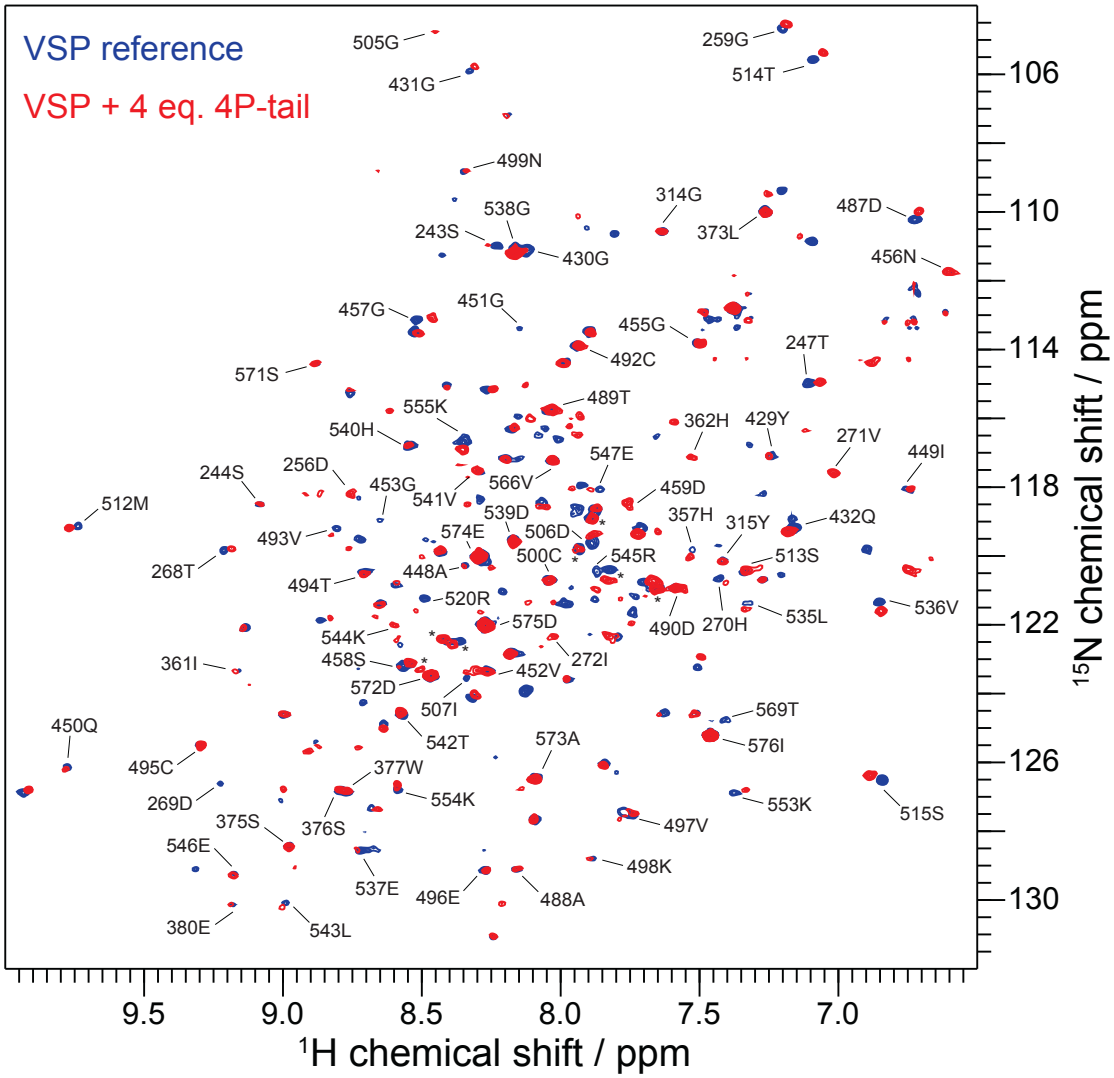

Figure S4. Assigned NMR spectrum of VSP with tetra-phosphorylated C-tail. Overlay of ^{15}N-^{1}H-HSQC spectra of VSP alone (blue) and VSP in the presence of 4 molar equivalent of PTEN C-tail (red). Peak assignments are shown.

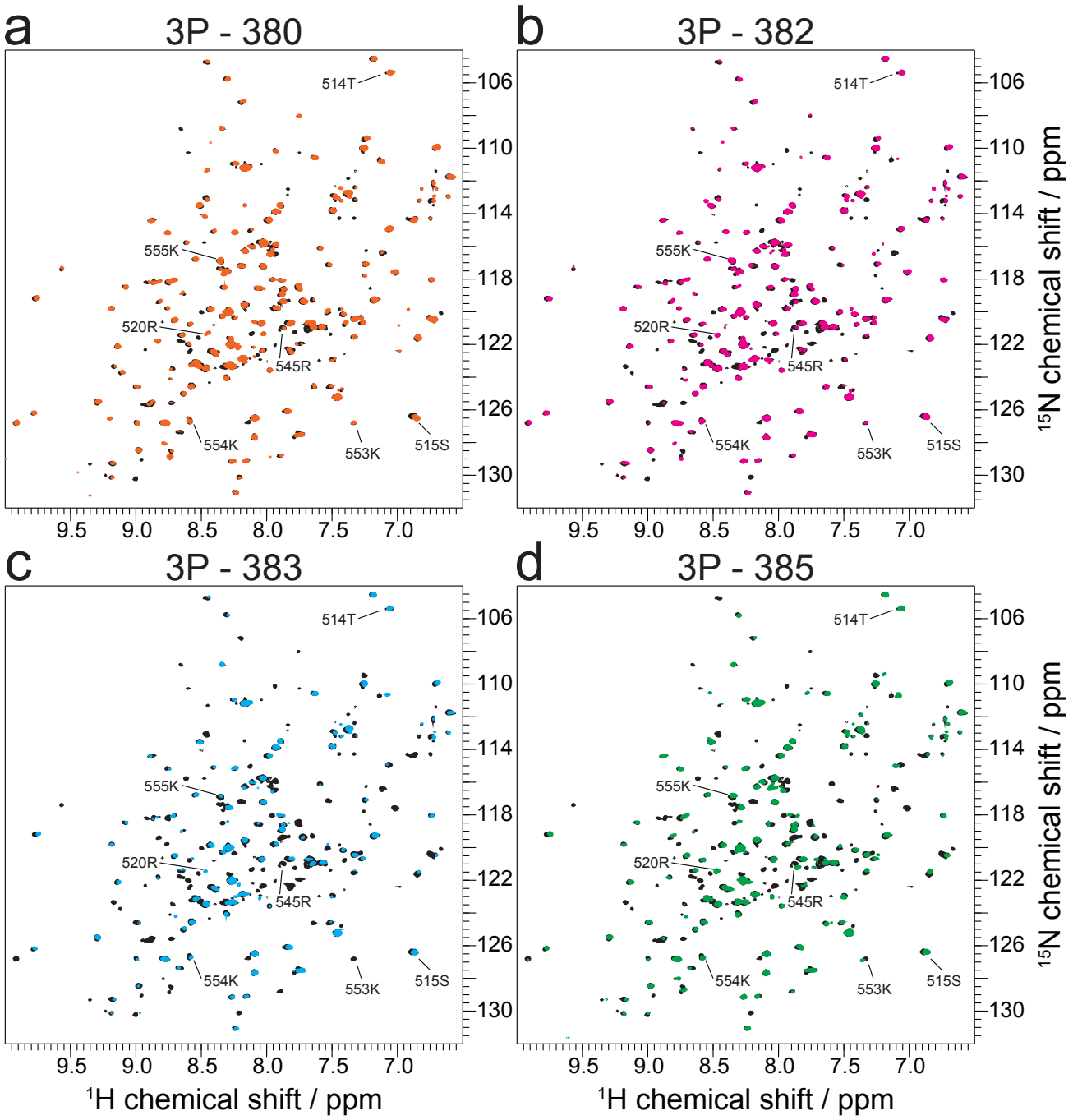

Figure S5. NMR spectra of VSP with tri-phosphorylated variants of C-tail. a-d, Overlay of ^{15}N-^{1}H-HSQC spectra of VSP in the presence of 1 molar equivalent of tetra-phosphorylated C-tail (black) and VSP in the presence of 1.2 molar equivalent tri-phosphorylated lacking pSer380 (a, orange), 1.2 molar equivalent tri-phosphorylated lacking pSer382 (a, magenta), 1.2 molar equivalent tri-phosphorylated lacking pSer383 (c, cyan) and 1.2 molar equivalent tri-phosphorylated lacking pSer385 d, green. Select assignments corresponding to residues in the CBRIII and Cα2 loops are shown.

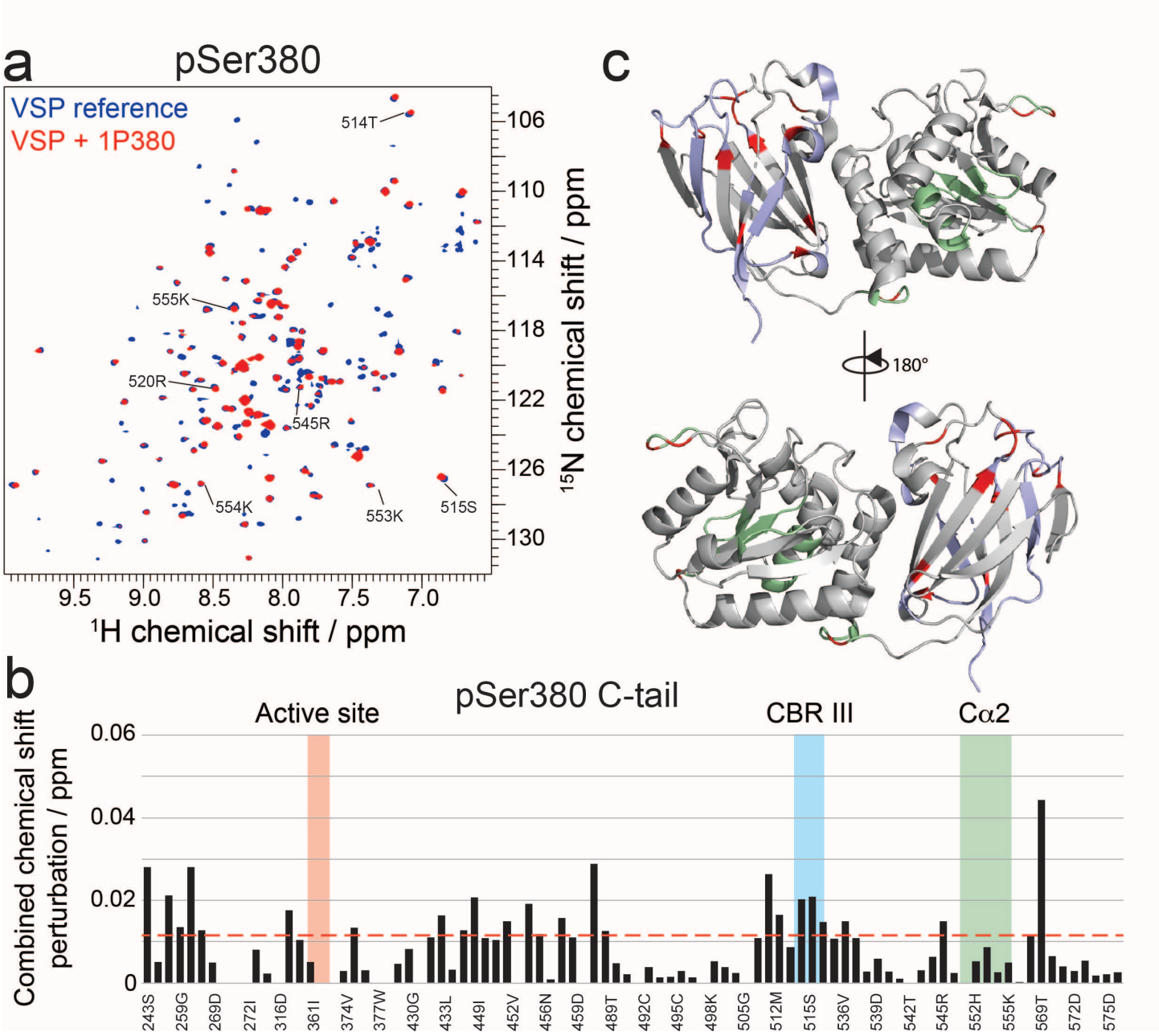

Figure S6. Mode of interaction of mono-phosphorylated PTEN C-tail with VSP. a, Overlay of ^{15}N-^{1}H-HSQC spectra of VSP alone (blue) and VSP in the presence of 4 molar equivalent mono-phosphorylated PTEN C-tail at position Ser380 (red). Selected residues of the CBRIII and Cα2 loops are showed with arrows. b, Combined chemical shift perturbations corresponding to spectra in (a) and plotted against VSP primary sequence. Dashed red line corresponds to the standard deviation to the mean, excluding outliers (higher than 3xSDM). Notable regions of VSP for their strong interaction or biological relevance are shown in colored areas. c, Structure of VSP (PDB:3V0G) colored according to NMR results. Unassigned residues are in grey. Assigned residues that do not experience significant chemical shift perturbations or peak intensity changes are shown in light blue for the C2 domain and light green for the catalytic domain. Residues that show significant perturbations are shown in red.

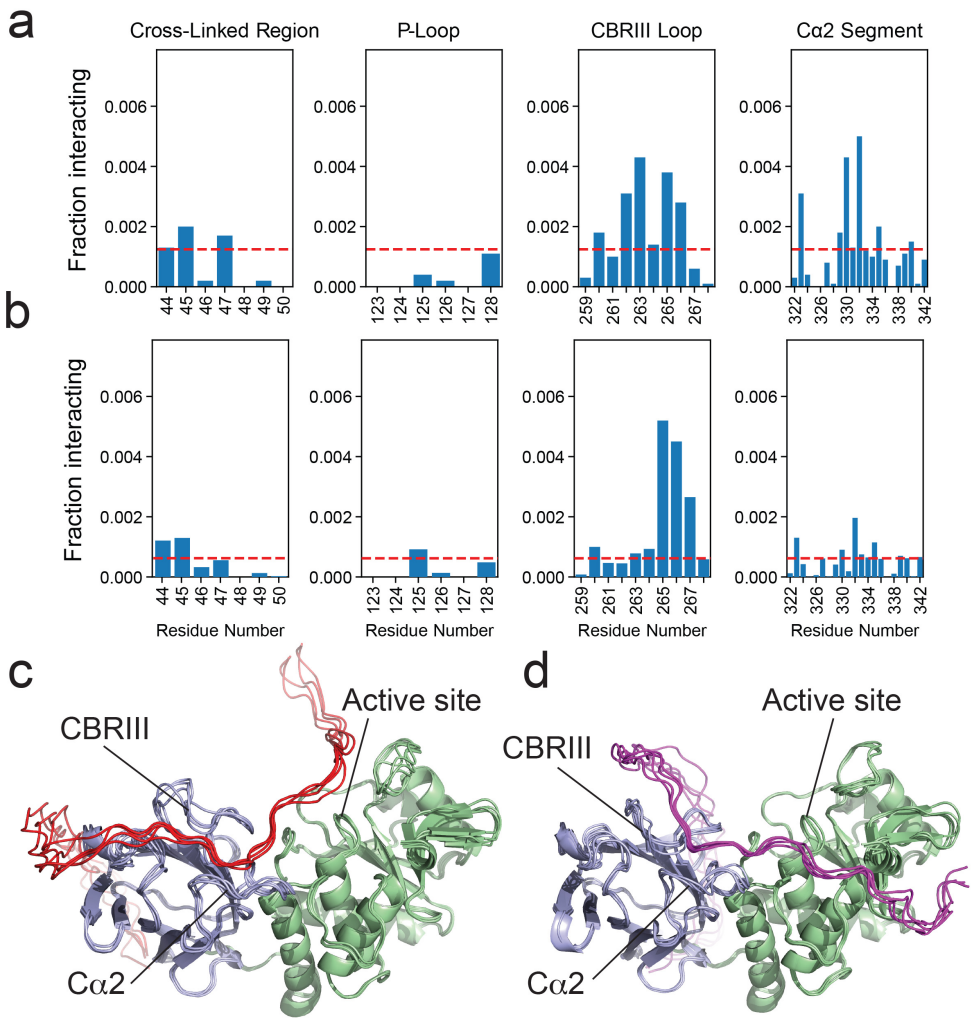

Cluster 1	
HADDOCK score	-452.5 +/- 5.0
Population	91%
RMSD	1.0 +/- 0.6
Van der Waals	-65.6 +/- 13.6
Electrostatic	-1224.2 +/- 46.0
Desolvation	19.5 +/- 2.1
Restraints violation	816.2 +/- 41.0
Buried surface area	2921.3 +/- 182.8
Z-score	-1.0

Cluster 2	
HADDOCK score	-406.0 +/- 10.9
Population	9%
RMSD	9.3 +/- 0.2
Van der Waals	-37.0 +/- 3.6
Electrostatic	-1080.5 +/- 108.5
Desolvation	28.3 +/- 3.1
Restraints violation	1212.8 +/- 53.2
Buried surface area	2913.4 +/- 69.7
Z-score	1.0

Figure S7. Modeling of tail:core interactions. a, Fraction of phosphorylated residues S380, T382, T383, S385 interacting with core residue X in regions of interest. The red line indicates the mean number of interactions across all models. Models were generated using the standard FloppyTail protocol. The phosphorylated residues show an above average preference for interacting with the CBRIII loop and the Cα-2 segment. b, Fraction of phosphorylated residues S380, T382, T383, S385 interacting with core residue X in regions of interest. The red line indicates the mean number of interactions across all models. Models were generated using fragments and constraints. The phosphorylated residues show an above average preference for interacting with the CBRIII loop and Cα-2 segment. c-d, Model of the complex created by HADDOCK (started from PDB:3V0G). The C2 domain is depicted in light blue and the catalytic domain in light green. Biologically important regions of VSP are pointed out. Top scoring HADDOCK cluster is shown in red (panel c) and the other in purple (four best structures, panel d). Their respective scores and statistical parameters are shown.

a

Protein	Ligand	K_d (μM)
VSP-NΔ16	F-4p-T4[#]	8.7 ± 0.3

[#] F-4p-T4 - CSDTTDSDPENEPFDEDK$_{fluorescein}$G

b

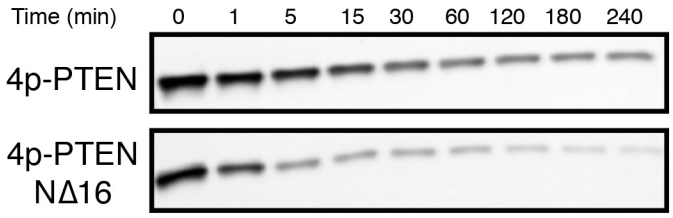

Figure S8. N-terminal helix has role in phospho-tail binding. a, Fluorescence anisotropy binding assay for VSP-NΔ16. Assay conditions: 50 mM Tris pH 8.0, 50 mM NaCl, 1 mM TCEP, n=2. b, Alkaline phosphatase sensitivity assay for 4p-PTEN-NΔ16. Assay conditions: 50 mM Tris pH 8.0, 10 mM 2-mercaptoethanol, 1 μM corresponding PTEN, and 2.7 U of alkaline phosphatase, n=3. Half-life for 4p-PTEN = 80 ± 30 min and 4p-PTEN-NΔ16 = 6 ± 3 min. Half-life for each protein is normalized to 1 U of alkaline phosphatase.